

## An investigation of the microstructures and properties of metal inert gas and friction stir welds in aluminum alloy 5083

A R YAZDIPOUR<sup>1,\*</sup>, A SHAFIEI M<sup>2</sup> and H JAMSHIDI AVAL<sup>2</sup>

<sup>1</sup>Welding Engineering Group, Metallic Materials Research Center, Malekashatar University of Technology, Tehran 15875-1774, Iran

<sup>2</sup>Department of Materials Science and Engineering, Sharif University of Technology, Tehran 11155-9466, Iran

e-mail: alireza.yazdipour@gmail.com

MS received 15 May 2010; revised 13 January 2011; accepted 22 March 2011

**Abstract.** Two different types of welds, Metal Inert Gas (MIG) and Friction Stir Welding (FSW), have been used to weld aluminum alloy 5083. The microstructure of the welds, including the nugget zone and heat affected zone, has been compared in these two methods using optical microscopy. The mechanical properties of the weld have been also investigated using the hardness and tensile tests. The results show that both the methods could successfully be used to weld such alloy. The strength of the joints is comparable to the strength of the base metal in both cases. However, FSWed samples have shown higher strength in comparison to the MIG samples. The results also show that the extension of the heat affected zone is higher in the MIG method in comparison to the FSW method. The weld metal microstructure of MIG welded specimen contains equiaxed dendrites as a result of solidification process during MIG welding while FSWed samples have wrought microstructures.

**Keywords.** Friction stir welding; metal inert gas welding; aluminum alloy 5083; mechanical properties; microstructures.

### 1. Introduction

The difficulty of welding the high-strength aluminum alloys has inhibited the wide use of welded aluminum structures. The high-strength aluminum alloys usually exhibit poor weldability mostly due to solidification problems. These consequently results in undesirable mechanical properties of welded parts. Therefore, the conventional welding processes are inappropriate for aluminum alloys. Recently, friction stir welding (FSW) technique has overcome many problems encountered in the conventional welding of aluminum alloys as it is a solid state welding process. Thus, FSW has shown to be a promising technique for joining the difficult-weld materials such as

---

\*For correspondence



**Figure 1.** Geometry of the tool used in the present study.

aluminum alloys. In FSW, two pieces of sheet or thin plate are joined by inserting a specially designed rotating pin into the adjoining edges of the sheets to be welded and then moving it all along the seam (Buffa *et al.* 2006). Usually, FSW has been used for the joining of aluminum alloys. However, recently FSW has been successfully used for the joining of high melt-point materials such as different steels (Cui *et al.* 2007, Sato *et al.* 2007, Saeid *et al.* 2008) and Titanium (Lee *et al.* 2005).

Although much attention has been paid recently to investigate the FSW welding method, there have been few works regarding the comparison of this technique by fusion welding methods. Therefore, the main aim of the present work is to compare FSW by Metal Inert Gas (MIG) as a fusion welding method. Al5083 has been selected as the base materials, because it can be considered as an important structural material with a high degree of corrosion resistance and excellent mechanical properties. Moreover, one could find different research works regarding the FSW of Al5083 (James *et al.* 2003, Czechowski 2005, Lombard *et al.* 2008, Kim *et al.* 2008). Lombard *et al.* (2008) have studied the effect of FSW tool rotational speed and feed rate on mechanical properties and fatigue life in Al5083 (Lombard *et al.* 2008). Effects of weld tool travel speed on fatigue life of friction stir welds in 5083 Al alloy have been investigated by James *et al.* (2003). Czechowski (2005) studied on low-cycle fatigue of friction stir welded Al5058 and Al5059 alloys. Kim *et al.* (2008) have studied fatigue crack propagation behaviour of friction stir welded Al5083 and Al6061 alloys based on residual stress measurement and fractographic observation.

## 2. Experimental procedure

The material under investigation was a 5083-H321 commercial aluminum alloy under the form of rolled plates of 5 mm thickness with chemical composition 4.2%Mg—0.60%Mn—0.25%Si—0.15%Fe—0.09%Zn—0.09%Cr—0.06%Cu—0.02%Ti—Bal Al (wt%). 200 mm × 75 mm large

**Table 1.** FSW tool dimensions.

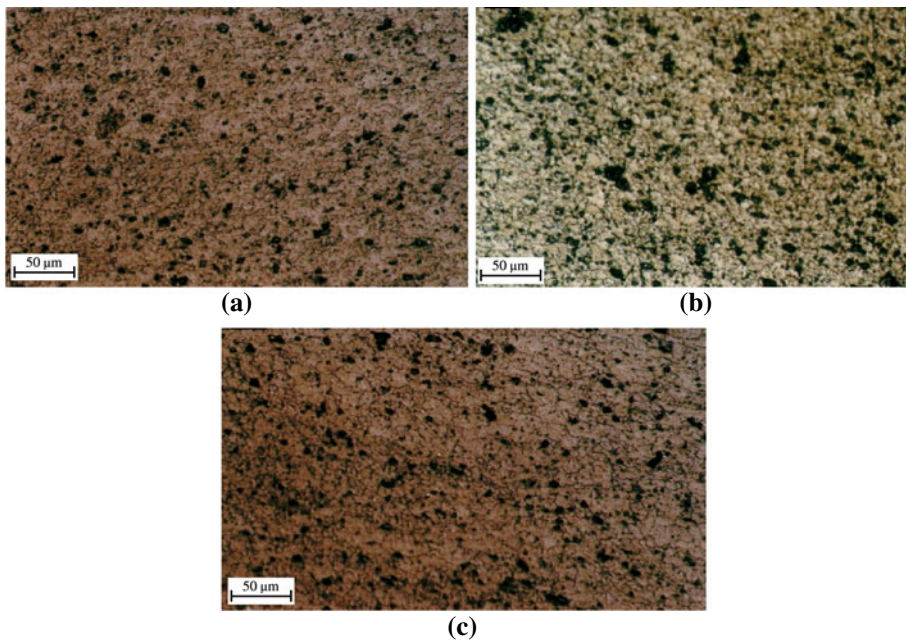
Tool dimensions	Values
Pin diameter, d (mm)	6
Shoulder diameter, D (mm)	18
Pin length, L (mm)	4.9
Tilt angle	3°

**Table 2.** Summary of FSW parameters used for Al5083-H321.

No.	$\omega$ (rpm)	$v$ (mm/min)
F-1	710	20
F-2	710	14
F-3	1000	28
F-4	1400	20

**Table 3.** Summary of MIG parameters used for Al5083-H321.

No	Travel speed (mm/sec)	Wire feed (m/min)	Voltage (V)	Amperage (A)	Heat input (j/mm)
M-1	7.8	8	20	145–150	290
M-2	7.8	8	18	136–143	304
M-3	7.8	9	20	160–170	323
M-4	7.8	10	20	178–182	367
M-5	8.77	9	20	160	378
M-6	10	9	22	170–175	379
M-7	7.24	8	18	120–125	423

**Figure 2.** Optical microscopic images of stir zone of FSWed specimens; (a) sample F-1, (b) sample F-2, (c) sample F-4.

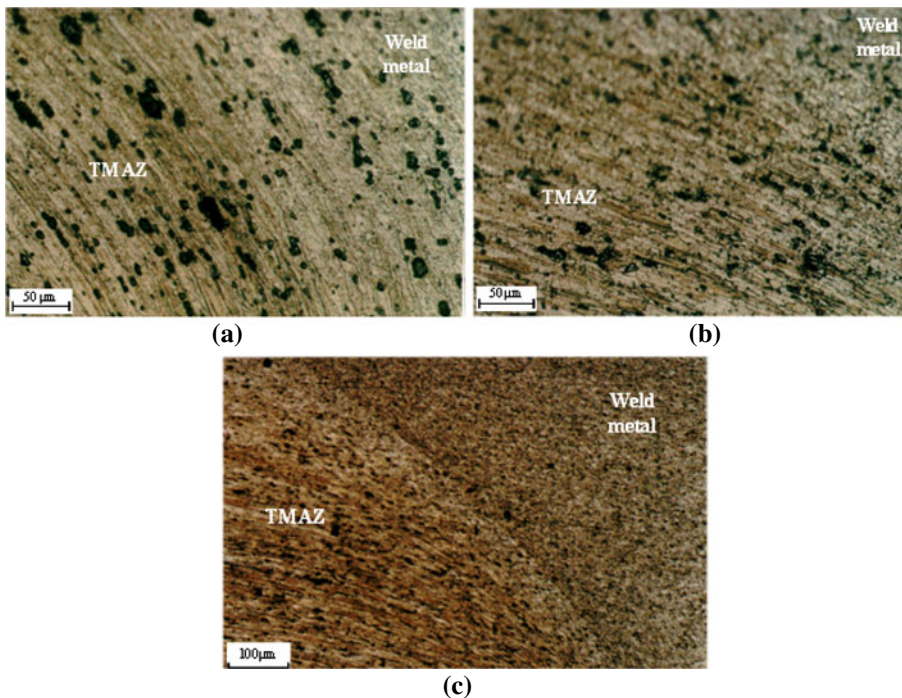


**Figure 3.** Optical microscopic image of (a) SZ and TMAZ of Sample F-1 in the retreating side and (b), (c) SZ and TMAZ of Sample F-4 in the advancing side after FSW.

plates were welded along the rolling direction. The plates were longitudinally butt-welded using a FSW machine. The FSW tool was a H13 tool steel in the quenched and tempered state with a threaded pin. The tool shape and its dimensions are shown in figure 1 and table 1 respectively. Welding parameters used for FSW are summarized in table 2.

Al5183 filler metal under protection of Argon was used to fabricate MIG welded joint in the same base material (Al5083-H321, 5 mm thickness). The conditions used for the MIG method are summarized in table 3. No pre-heat used in any condition, and root opening was 1.2 mm for all cases. The tensile test was performed for both the base metal and welded specimens. The tensile test specimens were cut perpendicular to the welding direction. In order to remove surface irregularities effect on tensile test results, all the weld samples were subjected to surface flat

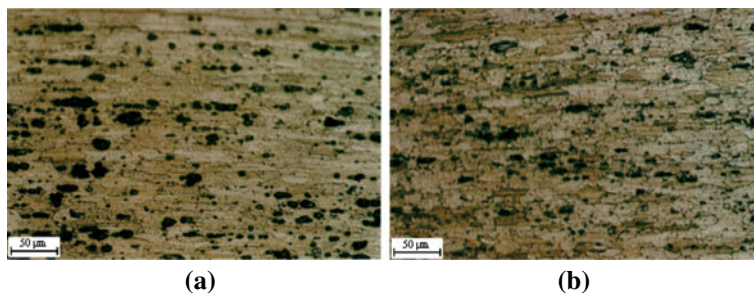


**Figure 4.** The HAZ microstructure of (a) sample F-1, (b) sample F-4.

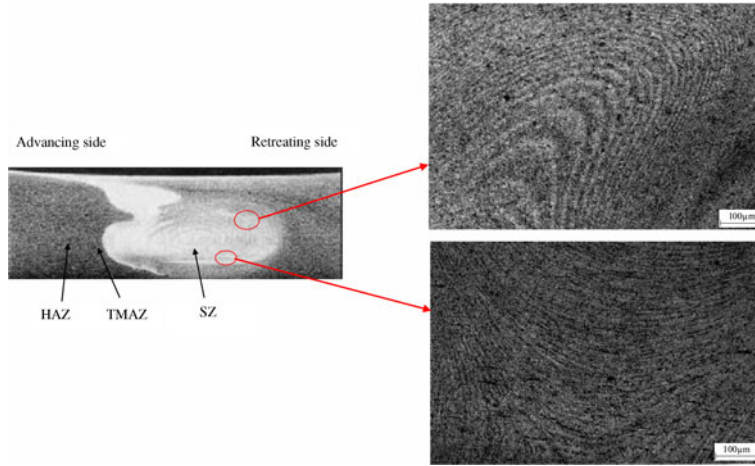


**Figure 5.** Onion rings structure observed in SZ of Sample F-4.

finishing before testing. The tensile test specimens were prepared according to ASTM E8M and performed using an INSTRON 1104 machine using constant cross-head speed of 2 mm/min. The Vickers micro-hardness of welded samples was measured using the hardness testing machine (Instron Wolpert). The hardness of base metal was measured to be about 130 HV, and the base metal tensile strength (UTS), yield strength and elongation were about 370 MPa, 154 MPa and 12%, respectively. The microstructures in the welded zone were observed by Optical Microscopy (OM). The polished cross-sectional processing specimens were chemically etched using Keller's reagent for 10 sec for the OM observations.

### 3. Results and discussions

#### 3.1 Microstructure

Cross-sections of the weld joints under the various FSW conditions were observed. Neither cracks nor porosity was visible, showing a good quality. Optical microscopic images of stir zone of FSWed specimens are shown in figure 2. The microstructure of the welded joint is formally divided into four zones (Lomolino *et al.* 2005): base material, heat affected (HAZ), thermo-mechanically affected (TMAZ) and stirred zone. The weld nugget is composed of fine-equiaxed recrystallized grains, which are formed under the high temperature and high rate of deformation

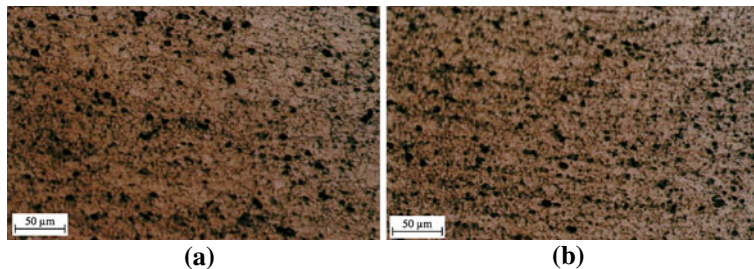


**Figure 6.** The microstructure of the stir zone in the; (a) upper surface, and (b) down side.

in the weld nugget due to the pin stirring (Kumar & Kailas 2008), and the size of the crystal grain is about  $8\ \mu\text{m}$  in different welding parameters (figure 2).

The TMAZ microstructure consists of bent elongated grains near the nugget shown in the micrograph of figure 3, and divided into the retreating side (RS) and the advancing side (AS). Although both the advancing side and the retreating side have a boundary with the weld nugget, the boundary in the advancing side is clearer than that in the retreating side. Beyond the TMAZ there is a heat-affected zone (HAZ) which is shown in figure 4. This zone experiences a thermal cycle, but does not undergo any plastic deformation (figure 4). The HAZ retains the same grain structure as the parent material. However, the thermal exposure has caused significant grain growth in this region with respect to SZ grain structure. The size of the crystal grain in HAZ is about  $20\ \mu\text{m}$  in different welding parameters.

Onion rings structure was observed in SZ of sample F-4 after FSW (figure 5). The main reason for observing this structure is differences in contrast between onion rings. The difference in

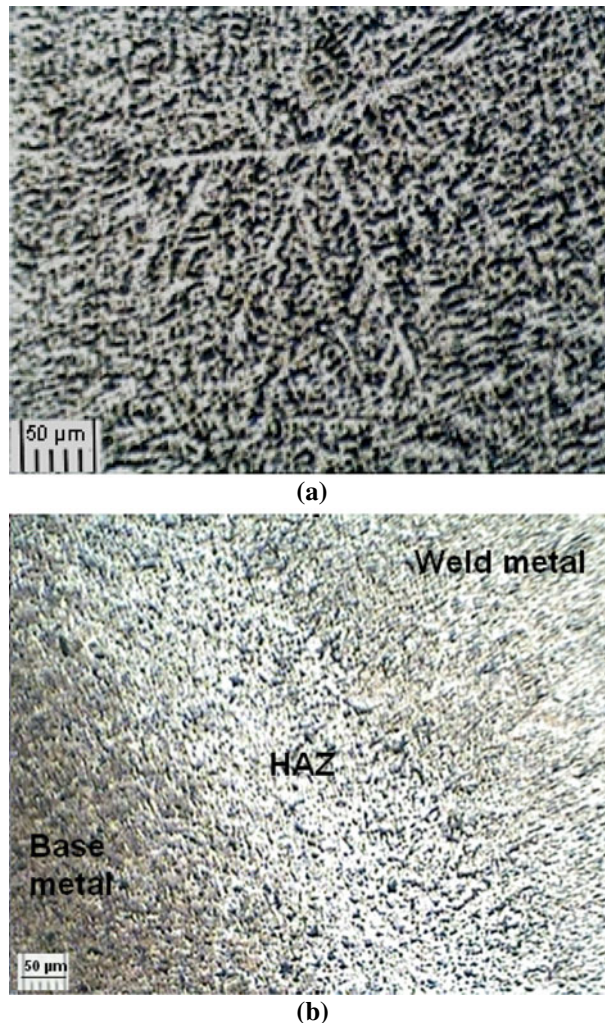


**Figure 7.** The microstructures of sample M-1; (a) weld metal, (b) weld metal, HAZ and base metal.

**Table 4.** The results of Vickers hardness for different samples.

No	F1	F-2	F-3	F-4			
HRD (VHN)	69	68.5	70	75			
No	M-1	M-2	M-3	M-4	M-5	M-6	M-7
HRD (VHN)	68	63	55.5	51	63	57.5	64.5

contrast between the onion rings is not due to variations in grain size or particle density, which implies that the onion ring structure in this alloy may be formed by texture variations.

Upper side and down side of stirred zone (SZ) of sample F-3 is exhibited in figure 6. It is clear that down side of SZ (figure 6b) in this sample has finer grain structure rather than upper side of this region. This diversity in SZ microstructure is as a result of extra frictional heat generated by friction between rotating shoulder and surface of specimen. The amount of this frictional heat is maximized in upper side of SZ, which is in direct contact with shoulder during the process. Consequently, the upper side grain structure is coarser than other sides of SZ.

Figure 7 shows the optical microscopic image of weld metal (WM) in MIG welded specimen. The WM microstructure of MIG welded specimen contains equiaxed dendrites as a result of solidification process during MIG welding. Based on this cast microstructure, it is predictable that FSW samples show better strengths. This has been described in the next section. It is worth noting that the defects (such as flaws and porosity) do not exist within the MIG welded specimen.

### 3.2 Mechanical properties

Table 4 shows the results of hardness measurements. It was mentioned previously that the base material is in an extremely work hardened state. The base material has a Vickers hardness of about 130 HV, very high for an alloy of this type. The hardness of FSWed samples is related to the hardness of the stir zone, whereas the hardness of MIG samples is related to the weld metal. Each hardness numbers in table 4 is the average of 10 separate hardness test. According to the table 4, it is clear that FSW welding process softens the material significantly with the hardness

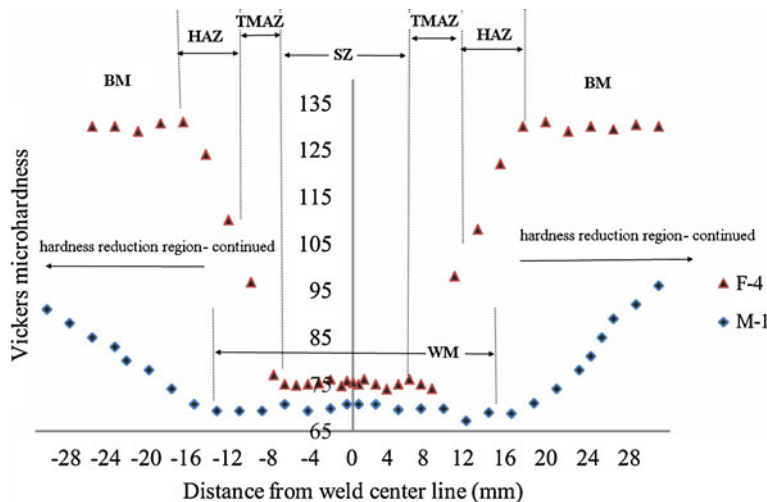


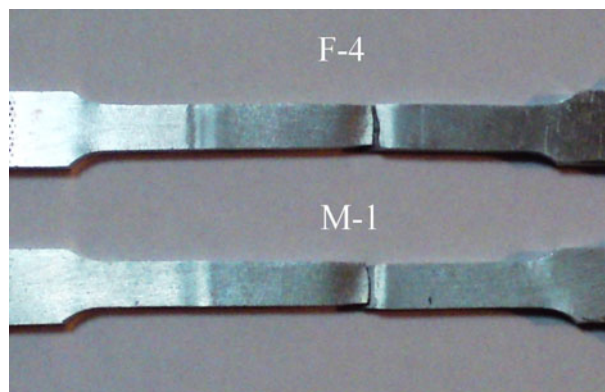
**Figure 8.** Micro-hardness profile of samples F-4 and M-1.

**Table 5.** The results of strengths for different samples.

No.	F1	F-2	F-3	F-4	M-1	M-2	M-3	M-4	M5	M-6
UTS	337.6	330	340	337	311	303	309	310	308	307
YS	138.6	133.9	140.1	141.6	133.9	130.9	126.2	126.4	127.2	126.1
Elongation%	20	20.4	19.7	19.4	15	16	15.2	16.3	16	15.2

reducing by nearly 50% around the weld line to about 75 HV. Figure 8 shows the horizontal hardness profiles across the joints of sample F-4 and M-1 measured at 2.5 mm from the root face. The variations in hardness mentioned above can be readily correlated with the microstructure developed both during and after the welding process. As stated above, the 5xxx series alloys are predominantly work hardenable alloys and so it is this microstructure, typical of rolling/work hardening that is the main contributor to the high hardness of this region compared to the weld zone (Kristensen *et al.* 2004; Uyyuru & Kailas 2006). It was shown that the welding process has dramatically altered the microstructure of the material in this region. The heavily worked microstructure of the base material has been completely replaced by equiaxed grains around 8  $\mu\text{m}$  in diameter that have little sub-structure, typical of a recrystallized microstructure and similar to that found previously in 5xxx, 6xxx and 7xxx series aluminum stir welds. In summary, it appears that the welding process essentially results in an annealed microstructure around the weld line with all the properties of 5083-O temper. The interesting point regarding the hardness of MIG samples is the fact that by increasing the heat input to the stir zone, the hardness has decreased. This can be due to this fact that by increasing the heat input to the WM, the grains in the WM will be coarser. As a result, the hardness will be lower for samples with higher heat inputs. In other words, by increasing the heat input to the stir zone the cooling rate will be decreased, and, as a result, the grains will have enough time for growth. Therefore, it can cause a decrease in the hardness.

The tensile strengths of samples with the efficiency of the welds are gathered in table 5. According to this table, it is clear that FSWed samples have shown higher hardness when compare to MIG samples. The FSWed specimens apparently represent an increase in properties relative to the MIG welded specimen of some 9–11% for ultimate tensile and yield strength. Also, the elongation of FSWed samples is about 16% higher than MIG samples. Generally, this improvement in mechanical properties can be explained by microstructural differences between

**Figure 9.** The tensile samples of F-4 and M-1 after fracture.

two joints. The optical microscopic images of weld metal (WM) in MIG welded specimen and FSWed specimen was demonstrated in figure 7. According to this figure, the WM microstructure of MIG welded specimen contains equiaxed dendrites as a result of solidification process during MIG welding. In contrast, stirred zone of FSWed specimen, evolves into fine equiaxed recrystallized grains under FSW condition as a result of dynamic recrystallization during FSW. In general, it is an accepted fact that finer grains could improve both hardness and strength of a metal according to the Hall–Petch relation. Therefore, higher strengths observed for FSWed samples could simply be related to their finer grains produced in the stir zone. It should be noted that the decrease in the strength in both FSWed and MIG samples is inevitable. That is because, as mentioned before, 5083-H321 is a non-heat treatable alloy; its hardening mechanism is therefore by work hardening or refining its structure. Therefore, heating the base metal due to FSW or MIG will modify the structure of the work-hardened base metal and it will decrease the strength. Moreover, it should be noted that increasing the heat input to the weld region will increase the extension of the HAZ zone, and will further decrease the strength of the weld. The pictures of the tensile samples of F-4 and M-1 after fracture in tension are shown in figure 9. By analysing the pictures it is possible to conclude that the both tensile samples of FSW and MIG experienced a straight failure, coincident with the axis of the soft weld region.

#### 4. Conclusions

Both fusion welding method (MIG) and solid state welding method (FSW) have been used for the welding of aluminum alloy 5083. The microstructure of the nugget zone and weld metal was compared in this two method, and it was concluded that while stir zone in the FSW samples is consisted of fine-equiaxed recrystallized grains, the weld metal of MIG samples is composed of dendrites formed during solidification. FSWed samples have shown higher strengths in comparison to the MIG samples, and that was related to structure of the stir zone in FSWed samples.

#### References

- Buffa G, Hua J, Shivpuri R, Fratini L 2006 A continuum based FEM model for friction stir welding-model development, *Materials Science and Eng. A*, 19: 389–396
- Cui L, Fujii H, Tsuji N, Nogi K 2007 Friction stir welding of a high carbon steel, *Scripta Materialia*, 56: 637–640
- Czechowski M 2005 Low-cycle fatigue of friction stir welded Al–Mg alloys, *J. Materials Processing and Technol.* 164–165: 1001–1006
- James MN, Hattingh DG, Bradley GR 2003 Weld tool travel speed effects on fatigue life of friction stir welds in 5083 aluminium, *Int. J. Fatigue*, 22: 1389–1398
- Kim S, Lee CG, Kim SJ 2008 Fatigue crack propagation behavior of friction stir welded 5083-H32 and 6061-T651 aluminum alloys, *Materials Science and Eng. A*, 478: 56–64
- Kristensen JK, Donne CD, Ghidini T, Mononen JT, Norman A, Pietras A, Russell M, Slater S 2004 *Proceedings of the Fifth International FSW Symposium*, Metz, France
- Kumar K, Kailas SV 2008 The role of friction stir welding tool on material flow and weld formation, *Materials Science and Eng. A*, 485: 367–374
- Lee WB, Lee C, Chang WS, Yeon YM, Jung SB 2005 Microstructural investigation of friction stir welded pure titanium, *Materials Letters*, 59: 3315–3318
- Lombard H, Hattingh DG, Steuwer A, James MN 2008 Optimising FSW process parameters to minimise defects and maximise fatigue life in 5083-H321 aluminium alloy, *Eng. Fracture Mech.* 75: 341–354

- Lomolino S, Tovo R, Santos J 2005 On the fatigue behavior and design curves of friction stir butt-welded Al alloys, *Int. J. Fatigue*, 27: 305–316
- Saeid T, Abdollah-zadeh A, Assadi H, Malek Ghaini F 2008 Effect of friction stir welding speed on the microstructure and mechanical properties of a duplex stainless steel, *Materials Science and Eng. A*, 496: 77–89
- Sato Y S, Yamanoi H, Kokawa H, Furuhashi T 2007 Microstructural evolution of ultrahigh carbon steel during friction stir welding, *Scripta Materialia*, 57: 557–560
- Uyyuru R K, Kailas S V 2006 Numerical analysis of friction stir welding process, *J. Materials Eng. and Performance*, 15: p. 505–518